Contact Angle Relaxation during the Spreading of Partially Wetting Drops

ARTICLE *in* LANGMUIR · DECEMBER 1997

Impact Factor: 4.46 · DOI: 10.1021/la970825v

Contact Angle Relaxation during the Spreading of Partially Wetting Drops

M. J. de Ruijter and J. De Coninck*

Université de Mons-Hainaut, Centre de Recherche en Modélisation Moléculaire, 20 Place du Parc, 7000 Mons, Belgium

T. D. Blake, A. Clarke, and A. Rankin

Kodak European R & D, Kodak Limited, Harrow HA1 4TY, U.K.

Received July 23, 1997. In Final Form: October 9, 1997[⊗]

We apply the molecular kinetic theory of wetting to the relaxation of the dynamic contact angle during the spreading of liquid droplets on solid surfaces. Experimental data have been obtained for several solid−liquid combinations and are successfully fitted using the theory. Physical parameters are extracted and interpreted in terms of the microscopic characteristics of the liquid and the solid. We also show that droplet spreading and forced wetting can be described by the same equations. A comparison is made between the results obtained within the molecular-kinetic framework and those obtained with conventional hydrodynamic theory.

Introduction

A dynamic contact angle, different from the equilibrium contact angle, is formed at a moving liquid meniscus in contact with a solid.[1] The liquid meniscus can be forced to move, for example by plunging a rod or a plate into the liquid. Alternatively, interfacial forces may drive the front spontaneously toward equilibrium. This is the case for a liquid drop spreading on top of a flat substrate, where the time-dependent contact angle, θ, relaxes from a possible maximum of 180° down to its equilibrium angle, $\theta^0 > 0$ in the case of partial wetting or zero if the liquid wets the solid completely. In practice, where the system exhibits contact angle hysteresis, the limiting value may be larger than the equilibrium angle.

To describe the dynamics of wetting, two different theoretical approaches have been proposed: one based on molecular kinetics and the other on continuum hydrodynamics. In the first,[2,3] wetting is described in terms of the kinetics of molecular processes occurring within the three-phase wetting zone. Blake and Haynes[3] view the progression of the wetting line as an adsorption/desorption process. Molecular displacements occur randomly but progressively as the wetting line advances. The theory links microscopic quantities such as the frequency and length of molecular displacements with the macroscopic, dynamic behavior of the contact angle. The dynamic behavior results from the balance between the driving force for wetting and the energy dissipation within the three-phase zone. The driving force is supposed to be the unbalanced capillary force arising from the change in the contact angle from its equilibrium value to some dynamic value, $\theta = \theta(v)$.

Although the theory was developed originally for forced wetting and experimentally verified in partial wetting regimes over a broad range of velocities,[3−5] it is expected to be appropriate equally to the spontaneous spreading of liquid droplets.[6] The specific aim of the present paper is to reconsider the molecular-kinetic theory within the context of droplet spreading.

According to the hydrodynamic theory of wetting, as exemplified by Voinov,[7] Hocking and Rivers,[8] and Cox,[9] the behavior of the dynamic contact angle arises primarily as a result of viscous bending of the fluid−fluid interface in the vicinity of the wetting line. Similarly, when hydrodynamics is applied to the spreading of liquid droplets, as for example in refs 7, 8, and 10−19, the evolution with time results from the interplay between the unbalanced capillary forces and the viscous resistance to flow. Most of the proposed models assume a quasi-stationary regime with small capillary number ($\mu U/\gamma_{LV}$) and small Reynolds numbers ($\rho RU/\mu$), where μ, ρ, and γ_{LV} are, respectively, the viscosity, density, and surface tension of the liquid and U is the spreading velocity for a droplet of radius R. Under these conditions, interfacial tension effects dominate viscous and inertial effects.

A major difficulty with conventional hydrodynamic theories of wetting is the singularity that results from the conflict between the classical no-slip boundary condition and a contact line that moves. In order to avoid this problem, the analysis is truncated a small distance from the wetting line.[7] Alternatively, the no-slip condition is relaxed in this region.[8,9]

The hydrodynamic models predict an apparent dynamic contact angle that differs from the local angle at the solid

[⊗] Abstract published in *Advance ACS Abstracts,* December 1, 1997.

(1) To form a meniscus, a second fluid has to be present. Here we will assume the displaced fluid does not influence the wetting dynamics of the displacing fluid. This assumption will hold for spreading drops if the displaced fluid is gaseous and if the adsorption to the solid is weak.

(2) Cherry, B. W.; Holmes, C. M. *J. Colloid Interface Sci.* **1969**, *29*, 174.
(3) Blake, T. D.; Haynes, J. M. *J. Colloid Interface Sci.* **1969**, *30*, 421.
(4) Hayes, R. A.; Ralston, J. *Langmuir* **1994**, *10*, 340.
(5) Blake, T. D. In *Wettability*; Berg, J. C., Ed.; Marcel Dekker: New York, 1993; p 251.
(6) Dodge, F. T. *J. Colloid Interface Sci.* **1987**, *121* (1), 154.
(7) Voinov, O. V. *Fluid Dyn.* **1976**, *11*, 714.
(8) Hocking, L. M.; Rivers, A. D. *J. Fluid Mech.* **1982**, *121*, 425.
(9) Cox, R. G. *J. Fluid Mech.* **1986**, *168*, 169.
(10) Yin, T. P. *J. Phys. Chem.* **1969**, *73*, 2413.
(11) Strella, S. *J. Appl. Phys.* **1970**, *41*, 4242.
(12) Ogarev, V. A.; Timonina, T. N.; Arslanov, V. V.; Trapeznikov, A. A. *J. Adhes.* **1974**, *6*, 337.
(13) Karnik, A. R. *J. Photogr. Sci.* **1977**, *25*, 197.
(14) Tanner, L. H. *J. Phys. D: Appl. Phys.* **1979**, *12*, 1473.
(15) Starov, V. M. *Colloid J. (Transl. of Kolloidn. zh.)* **1983**, *45* (6), 1009.
(16) de Gennes, P. G. *Rev. Mod. Phys.* **1985**, *57*, 827.
(17) Chen, J. D. *J. Colloid Interface Sci.* **1988**, *122* (1), 60.
(18) Diez, J. A.; Gratton, R.; Thomas, L. P.; Marino, B. *J. Colloid Interface Sci.* **1994**, *168*, 15.
(19) de Gennes, P. G.; Cazabat, A. M. *C. R. Acad. Sci.* **1990**, *310*, 1601.

S0743-7463(97)00825-1 CCC: $14.00

surface. This local angle is smaller than the apparent advancing contact angle and is usually assumed to have its static or equilibrium value. In completely wetting systems a precursor film or "foot" is formed in a local region which spreads just ahead of the bulk liquid. For nonpolymeric liquids, as discussed by de Gennes,[15] the foot is of mesoscopic scale and arises as a result of long-range van der Waals forces.

In the simplest cases, hydrodynamics leads to a simple cubic relationship between the contact angle and the capillary number—the so-called "Tanner's law" for spontaneous, complete spreading.[14] More general treatments are given by Voinov[7] and Cox.[9] For spreading drops, both approaches lead to similar predictions for the evolution of the apparent contact angle with time, and the resulting equations have been used successfully to fit data obtained under conditions of both partial and complete wetting.[7,8,20] Nevertheless, these hydrodynamic pictures are essentially continuum descriptions, which diverge at the wetting line. This is an indication that processes appearing at the microscopic scale are potentially important. Very recently, a new hydrodynamic theory of wetting dynamics has appeared in which this is formally acknowledged.[21,22] In this paper, we will compare the predictions of the molecular-kinetic and conventional hydrodynamic theories with experiment.

Let us first recall the molecular-kinetic theory. According to Blake and Haynes,[3] the macroscopic behavior of the wetting line depends on the overall statistics of the individual molecular displacements which occur close to the wetting line. The velocity of the wetting line is characterized by K, the frequency of the molecular displacements, and λ, the typical length of each molecular displacement. In simple cases, λ is the distance between two neighboring adsorption sites on the solid surface. If K_{net} is the net frequency resulting from molecular displacements in the direction of wetting, K^+, and in the reverse direction K^-, such that $K_{net} = K^+ - K^-$, then the velocity of the wetting line is given by

$$v = (K^+ - K^-)\lambda = K_{net}\lambda \tag{1}$$

At equilibrium, $K_{net} = 0$ and $K^+ = K^- = K^0$, where K^0 is the quasi-equilibrium frequency. Blake and Haynes assumed the driving force to be the out-of-balance surface tension force $\gamma_{LV}(\cos(\theta^0) - \cos(\theta))$, where γ_{LV} is the surface tension of the liquid. Using Eyring's activated-rate theory for transport in liquids, they found the following relationship between θ and v:

$$v = 2K^0\lambda \sinh\left[\frac{\lambda_{LV}}{2nk_BT}(\cos(\theta^0) - \cos(\theta))\right] \tag{2}$$

where n is the number of adsorption sites per unit area, k_B is Boltzmann's constant, and T is the temperature.[23] This theory is independent of geometry.

For normal liquids, the capillary number for a spreading drop will be small. If the drop is small, then the effect of gravity on drop shape can be neglected. Thus, the shape of the drop will approximate a spherical cap.[22] These conditions pertained in all our experiments. The geometry of a spherical cap is characterized by the following relationship:

$$r = \left(\frac{3V}{\pi}\frac{\sin^3(\theta)}{2 - 3\cos(\theta) + \cos^3(\theta)}\right)^{1/3} \tag{3}$$

where V is the volume of the drop, r is the base radius, and θ is the instantaneous dynamic contact angle. For liquids of low volatility, V is constant; hence

$$\frac{\partial r}{\partial t} = \frac{\partial r}{\partial \theta}\frac{\partial \theta}{\partial t} \tag{4}$$

and we can derive the following:[24,25]

$$\frac{\partial r}{\partial t} = v = -\frac{\partial \theta}{\partial t}\left(\frac{3V}{\pi}\right)^{1/3}\frac{(1 - \cos(\theta))^2}{(2 - 3\cos(\theta) + \cos^3(\theta))^{4/3}} \tag{5}$$

Equations 2 and 5 are effectively a linked pair of partial differential equations with two unknown adjustable parameters:

$$\begin{cases} a = 2K^0\lambda \\ b = \dfrac{\lambda_{LV}}{2nk_BT} \end{cases} \tag{6}$$

The limiting value of the dynamic contact angle (assumed equal to θ^0) may also be treated as an unknown. The equations can be solved numerically to give the time evolution θ(t) and to find the best parameters a, b, and θ^0 to fit a given set of experimental spreading data.

In our analysis, the differential equations were first solved with a fourth-order Runge-Kutta algorithm;[26] then the difference between experimental data and the theoretical curve was minimized using the downhill simplex method.[26,27] As will be shown below, we have used this procedure to fit experimental data for several combinations of liquids and solids and found excellent agreement. We have also found that droplet spreading is described by the same parameters as forced wetting.

For completeness, let us now reconsider how the hydrodynamic theory may be applied in the same situation. For small capillary numbers,[9]

$$g(\theta) = g(\theta^0) + \frac{v\mu}{\lambda_{LV}}\ln\left(\frac{r}{s}\right) \tag{7}$$

where $g(q)$ is a complex integral function. The slip length s, which is introduced by the slip condition near the wetting line, is expected to be of the order of molecular dimensions.[20] For the later stages of spreading, when the contact angle is less than $3\pi/4$, eq 7 approximates to

$$\theta^3 = (\theta^0)^3 + 9\frac{v\mu}{\lambda_{LV}}\ln\left(\frac{r}{s}\right) \tag{8}$$

where we assume that the contact angles are the experimentally accessible ones. Combining eqs 5 and 8 leads to

(20) Cazabat, A. M. *Adv. Colloid Interface Sci.* **1992**, *42*, 65.
(21) Shikhmurzaev, Yu. D. *Sov. Phys. Dokl.* **1991**, *36*, 749; *J. Fluid Mech.* **1997**, *334*, 211.
(22) Shikhmurzaev, Yu. D. *Phys. Fluids* **1997**, *9*, 266.
(23) Note that the factor 2 in the denominator of the argument of sinh was omitted in the original formulation.[3]
(24) Blake, T. D.; Clarke, A.; De Coninck, J.; de Ruijter, M. J. *Langmuir* **1997**, *13*, 2164.
(25) Note that in a previous publication the factor $(3V/\pi)^{1/3}$ was omitted in eq 3.
(26) Press, W. H.; Teukolski, S. A.; Vetterling, W. T.; Flannery, B. P. *Numerical Recipes*, 2nd ed.; Cambridge University Press: New York, 1992.
(27) In fact, by integrating the equations, a fourth parameter is introduced. This parameter (*e.g.* the dynamic contact angle at time 0) was simultaneously fitted with a, b, and θ^0.

$$\frac{\partial\theta}{\partial t} = A^{-1}(\theta^3 - (\theta^0)^3)\frac{(2 - 3\cos(\theta) + \cos^3(\theta))^{4/3}}{(1 - \cos(\theta))^2} \quad (9)$$

with

$$A = -9\frac{\mu}{\lambda_{LV}}\ln\left(\frac{r}{s}\right)\left(\frac{3V}{\pi}\right)^{1/3} \quad (10)$$

This is similar to Voinov's eq 4.4.[7] The expression for A can be found by fitting experimental data. Here, we have fit the same experimental data to both the molecular-kinetic theory and eqs 9 and 10.

Materials and Methods

A drop of liquid brought in contact with a solid surface will spontaneously spread until it has relaxed to its static configuration. In the absence of contact angle hysteresis, this configuration is prescribed by the equilibrium contact angle. In our experiments (Figure 1), we fixed the needle of a syringe containing the liquid just above the substrate, so that a drop falling from the tip of the needle immediately touched the solid surface and began to spread. The liquid in the syringe was displaced by a high-precision screw, enabling us to calculate the volume of the drop from the displacement of the syringe plunger. The solid substrates were attached by double-sided tape to a glass slide and mounted horizontally.

The spreading of the drops was captured, from the moment they detached from the needle, by a video recorder connected to a CCD camera and a microscope. The drops were back-lighted. With this method, we were able to capture 50 images of the relaxing drop per second. From each consecutive image, the edge of the drop and its reflection were located with a common Sobel edge detector.[27] The drop profile close to the three-phase zone was then interpolated with a circular fit. The contact angle was determined at the point where the fit to the drop and its reflection intersected. This procedure was done automatically for each image using a program written within LabView. With this arrangement it was possible to measure contact angle relaxation directly over a long period of time with high resolution.

Our experiments were performed with glycerol−water solutions, di-*n*-butyl phthalate (DBP), and squalane (2,6,10,15,19,23-hexamethyltetracosane). The glycerol was supplied by Fisher (SLR grade, 98%), and the DBP by Fisons (SLR grade, 99%). The squalane was supplied by Sigma. The water used to make the glycerol solutions was purified in a Milli-Q system. The drops were deposited on a poly(ethyleneterephthalate) (PET) Kodak *Estar* film and clean glass microscope slides (Chance), which were used as received.

Table 1 shows the viscosity and surface tension of the liquids, measured at 21 °C, the ambient temperature during the experiments. We used two glycerol−water solutions of different concentrations to measure the effect of the viscosity on the fitted parameters. For each liquid, measurements were made with several drops of slightly different volumes (from 5.0 mm^3 to 9.5 mm^3).

Forced wetting measurements of DBP on PET over a range of speeds were performed by drawing a 35 mm wide PET film vertically into a bath of DBP. For each imposed velocity, the corresponding dynamic contact angle was measured directly from video images.

Results and Discussion

1. Droplet Spreading. Figure 2 shows our measurements of droplet relaxation. As can be seen from Figure 2a and b, the glycerol−water solutions exhibited a large equilibrium contact angle with PET and relax very rapidly. Within the first second the drop spread from its first measurable contact angle (around 90°) to nearly its equilibrium angle. Figure 2c−e reveal that squalane and DBP initially spread faster on both substrates. The first clear images that could be analyzed revealed a dynamic contact angle lower than that for the glycerol−water solutions. However, the later relaxation was slower. After 4 s of spreading, a small change in contact angle could still be observed, while for the glycerol−water solutions the drops stopped spreading by this time.

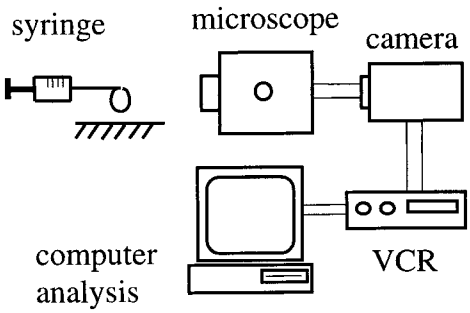

Figure 1. Schematic view of the experimental setup.

Table 1. Viscosity and Surface Tension of Liquids Used in Relaxing Contact Angle Measurements

liquid	composition[a] (% glycerol)	viscosity (mPa·s)	surface tension (mN/m)
glycerol (1)	90.1	209.0	65.3
glycerol (2)	88.3	156.0	65.7
squalane		29.0	30.7
DBP		19.6	34.3

[a] Glycerol−water in weight percent.

2. Molecular-Kinetic Theory. The evolution of the contact angle was fitted by solving the two partial differential equations (eqs 2 and 5), with a, b, and θ^0 as parameters. By way of example, Figure 3 shows an experimental curve for a spreading drop of DBP and its best fit. As can be seen, the fit is of excellent quality. We calculated the error function as follows:

$$E = \frac{1}{N}\sum_{i=1}^{N}\left(\frac{\theta_i^T - \theta_i^E}{\sigma}\right)^2 \quad (11)$$

with N the number of experimental data points, σ the estimated error per measurement (about 1°), and θ^T and θ^E the theoretical and experimental dynamic contact angle, respectively. This error function is a measure for the 'goodness' of the model. In all our fitting procedures, we found values less than 1, indicating that the molecular-kinetic theory models the spreading data well.

The resulting parameters for all the liquid−solid systems are given in Table 2. To estimate the errors on the parameters, we applied the "bootstrap" method.[26] The original experimental data are used as the basis for a Monte Carlo simulation: from this original set, 37% (≈1/e) randomly chosen points are replaced by duplicates. The duplicate points are chosen according to a normal distribution function with the original point for the average and a given value as the standard deviation, in this case the estimated error on each measured datum point. In this way, we replace the original set of data with a new one, for which the corresponding parameters are then calculated. Successive calculations result in a simulated set of values for each parameter. For 300 cycles, these sets turned out to be normally distributed, providing us with the mean value and standard deviation for each parameter. The values given in Table 2 are based on an estimated error of 1° on the measurement of the individual angles.

In spite of the large number of data per experiment and the goodness of the fit, the errors on the a and b parameters are significant. This is because the two parameters are not entirely independent. In Figure 4 the results for one Monte Carlo simulation are shown. It is clear that the

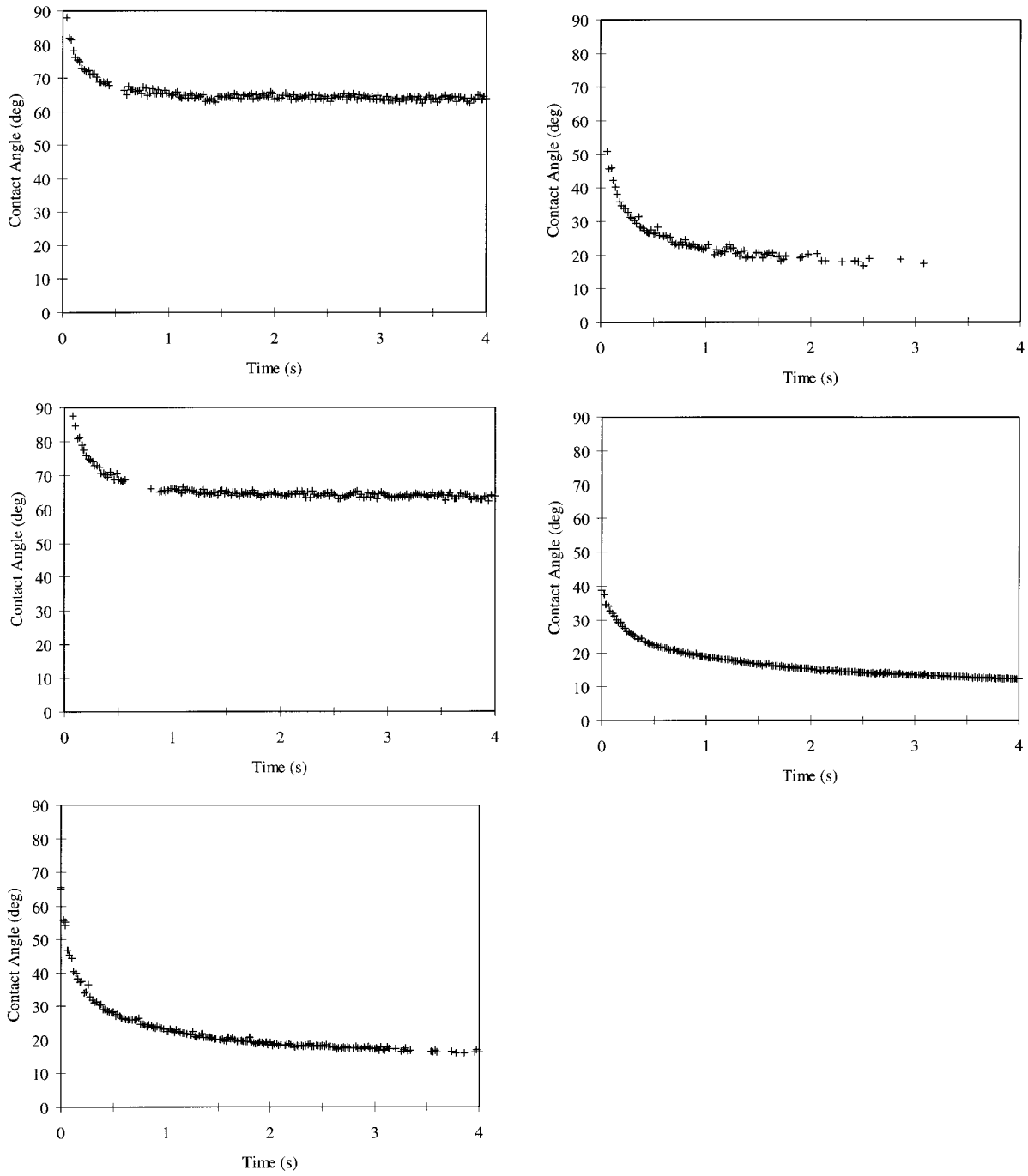

Figure 2. (a) Glycerol (1), (b) glycerol (2), and (c) squalane on PET and (d) squalane on glass and (e) DBP on PET.

errors on a and b are due to the connection that exists between them. Indeed, close to equilibrium eq 2 can be approximated by a linear relation between the velocity of the contact line and the capillary driving force.[3,5] The only significant parameter in that case is the product ab. Nevertheless, the actual values of a and b for the different liquid−substrate combinations are readily distinguishable and experimentally relevant. They yield the key microscopic parameters of wetting, namely the site density n, the average length of each molecular displacement $\lambda \approx 1/n^2$, and the frequency of displacements at equilibrium K^0. These are listed in Table 3, with errors calculated from those estimated for the fitting parameters.

Let us concentrate first on the site density and molecular displacement length. As expected, the different viscosities of the two glycerol−water solutions do not appear to have much influence on n or λ. On the other hand, by comparing the four different liquids on the same substrate, PET, it is clear that the nature of the liquid does have an influence. The results for squalane on PET and glass confirm this. In fact, the fitted values for λ are in quite good agreement with the dimensions of the liquids. For example, a simulation of a squalane molecule using the software Insight II 4.0.0 MSI reveals a radius of gyration of 7.9 ± 0.5 Å.

The equilibrium frequency K^0 is related to the effective molar activation free energy of wetting ΔG^*_w by

$$K^0 = \left(\frac{k_B T}{h}\right) \exp\left(\frac{-\Delta G^*_w}{N_A k_B T}\right) \qquad (12)$$

where h is Planck's constant and N_A is Avogadro's constant.[5] The corresponding specific activation free

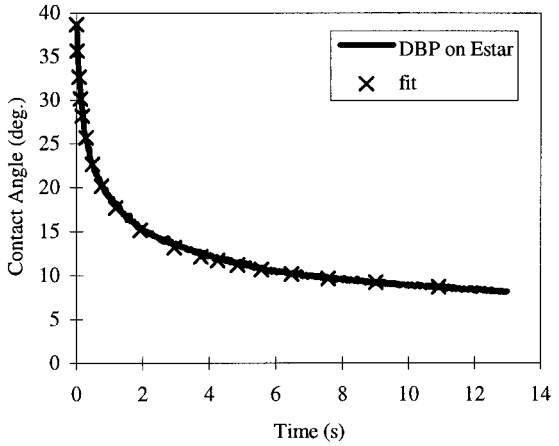

Figure 3. Experimental data and fit for DBP on PET.

Table 2. Parameters Resulting from Applying the Molecular-Kinetic Theory to the Data for the Various Liquid−Solid Systems

	a (10^{-2} cm/s)	b	θ^0 (deg)
glycerol (1) on PET	2.8 ± 0.2	9.6 ± 0.4	64.2 ± 0.1
glycerol (2) on PET	2.1 ± 0.2	9.2 ± 0.4	63.8 ± 0.1
squalane on PET	13.7 ± 0.5	4.5 ± 0.1	15.0 ± 0.1
DBP on PET	3.9 ± 0.2	13.3 ± 0.4	5.4 ± 0.2
squalane on glass	21.2 ± 0.4	4.5 ± 0.2	17.4 ± 0.2

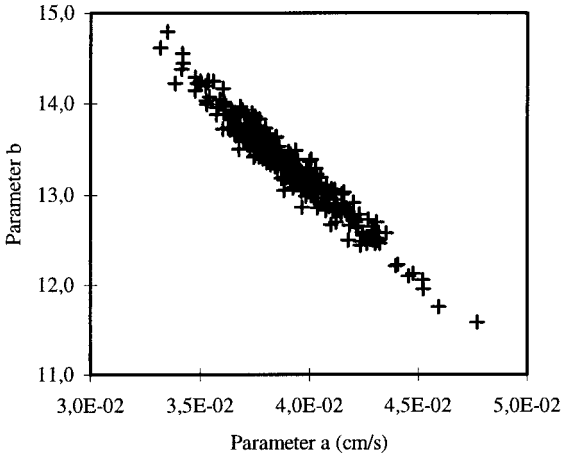

Figure 4. Estimation of the errors on a and b for DBP on PET.

energy of wetting (per unit area of the solid surface) is given by

$$\Delta g^*_w = \frac{n\Delta G^*_w}{N_A} \tag{13}$$

The experimental values of ΔG^*_w and Δg^*_w for the five systems studied are given in Table 3. The magnitudes of these quantities should be related to the energy required for the wetting line to move across the solid surface and, by implication, the strength of the molecular interactions that must be overcome. The values for the two glycerol solutions are almost the same, suggesting a rather weak effect of viscosity in these experiments. Comparing DBP and glycerol with squalane, it appears that glycerol and DBP interact somewhat more strongly with PET than squalane. This could be due to the presence of oxygen-containing polar groups in both DBP and glycerol. On the other hand, squalane interacts a little more strongly with PET than with glass, which may be due to the presence of adsorbed water vapor on the glass and stronger dispersion interactions between squalane and PET. Note, however, that when the effect of the adsorption site density is taken into account, the relatively low value of Δg^*_w for DBP on PET indicates that wetting proceeds more easily in this system than in the others studied.

For all the systems, the ΔG^*_w values reveal relatively strong interaction between the liquid and solid molecules within the three-phase zone. In comparison, an activation free energy of about 10 kJ/mol is expected for viscous flow in simple liquids.[5] Evidently, the values for the three-phase zone are significantly higher, and as a result the corresponding frequencies are much lower than would be expected in bulk flow. In these systems, therefore, surface effects are dominant. However, with increasing viscosity, we can expect the importance of surface effects to diminish.[2,5]

For liquids that completely wet the substrate, the disjoining pressure becomes a key variable, and the driving force for wetting can no longer be interpreted simply in terms of the surface tension and contact angle. Under these circumstances, a precursor film will form[18,19] and the hydrodynamic description of droplet spreading becomes more appropriate, since the wetting line is removed from the problem. Within these constraints, however, the molecular kinetic theory is self-consistent. In a recent article,[24] many of the assumptions underlying the theory have been validated by molecular dynamics simulations. These studies show not only that the theory is able to describe the dynamic behavior of the contact angle during partial wetting but also that the parameters used in the model are physically meaningful.

3. Forced Wetting. Figure 5 shows the steady-state dynamic contact angle of DBP on PET as a function of substrate velocity. Equation 2 has been used to fit the data and determine the values of a, b, and θ^0. The best fit is plotted in Figure 5, together with the results obtained by analyzing the corresponding relaxation data (angle versus instantaneous velocity $\partial r/\partial t$). If we simply compare the two curves, the velocity dependences of the contact angle in forced wetting and spontaneous spreading are clearly different. However, if we compare the fitting parameters, we see that a and b values are almost the same, and it is the values of θ^0 that differ. This discrepancy is probably due to contact angle hysteresis. In the forced wetting experiments, the contact angle observed when the PET tape is brought to a stop is the static advancing contact angle. On the other hand, the value for the contact angle measured with spreading droplets after a long time tends to fall below that value, becoming smaller than the advancing angle but remaining larger than the receding angle. Although one of the reasons for selecting PET as the substrate was its low roughness, some hysteresis cannot be avoided. As a result the experimentally observed static contact angles will always depend to some extent on the history and geometry of the system. With a Wilhelmy balance we measured an advancing angle of 16° and a receding angle of 0° for DBP. With the spreading drop, the angle took an intermediate value, 5.4°.

The fact the parameters a and b are comparable under conditions of forced wetting and spontaneous spreading indicates that the behavior of the dynamic contact angle is independent of the source of motion. It also implies that it is valid to use the same model of wetting in both circumstances and that the distinction between the two modes of wetting is probably artificial—a view also developed at some length by Shikhmurzaev.[21]

4. Hydrodynamic Theory. The procedure used to fit the data to the molecular-kinetic theory was also used with the hydrodynamic model (eqs 9 and 10). Two unknown quantities were determined, namely the equilibrium contact angle and the logarithmic term, $\ln(r/s)$. The value of the error function (eq 11) was again smaller

Table 3. Molecular Parameters for the Different Liquid−Solid Systems

	n (10^{+17} m^{-2})	λ (10^{-9} m)	K^0 (10^{+5} L/s)	ΔG^*_w (kJ/mol)	Δg^*_w (mJ/m^2)
glycerol (1) on PET	8.4 ± 0.4	1.09 ± 0.03	1.3 ± 0.1	43.2 ± 0.2	60 ± 3
glycerol (2) on PET	8.8 ± 0.4	1.07 ± 0.03	1.0 ± 0.1	43.8 ± 0.3	64 ± 3
squalane on PET	8.4 ± 0.2	1.09 ± 0.02	6.3 ± 0.3	39.3 ± 0.2	55 ± 2
DBP on PET	3.2 ± 0.1	1.77 ± 0.03	1.1 ± 0.1	43.6 ± 0.2	23 ± 1
squalane on glass	8.3 ± 0.4	1.10 ± 0.04	9.6 ± 0.5	38.3 ± 0.1	52 ± 3

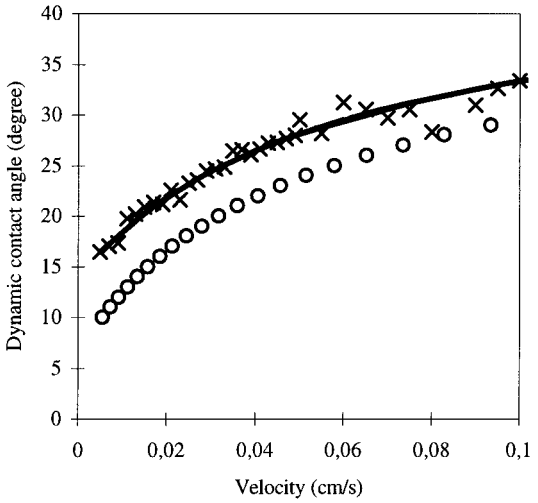

Figure 5. Dynamic contact angle of DBP in contact with PET. (×) Forced wetting data; the solid line is the best fit with a = 0.034 cm/s, b = 13.2, and θ^0 = 14.0°. (○) Data for droplet spreading; the best fit gives a = 0.039 cm/s, b = 13.3, and θ^0 = 5.4°.

Table 4. Fitting Parameters According to Eqs 9 and 10

	ln(r/s)	θ^0 (deg)
glycerol (1) on PET	44 ± 2	64.3 ± 0.1
glycerol (2) on PET	46 ± 3	63.9 ± 0.1
squalane on PET	24.8 ± 0.2	12.7 ± 0.1
DBP on PET	23.0 ± 0.1	0.0
squalane on glass	19.4 ± 0.2	15.6 ± 0.1

than 1, indicating that the data are well represented by eq 9. The results are given in Table 4. The errors were calculated with the same procedure as before. The equilibrium contact angles for the glycerol−water solutions are the same as those obtained with the molecular-kinetic theory, but the angles calculated for squalane and DBP are somewhat smaller. More significantly, the logarithmic terms are much larger than those found previously. Values of about 14 are usually reported.[20] Taking r to be of the order 0.1 cm yields values of s in the range 1×10^{-13} to 1×10^{-23} m. These values are entirely nonphysical and inconsistent with the continuum picture of wetting: a result which strongly suggests an additional source of energy dissipation within the three-phase zone in addition to the purely viscous one. This was already pointed out by Petrov and Petrov.[28]

Conclusions

In this article we have shown that the molecular-kinetic theory can be used successfully to describe contact angle relaxation during droplet spreading in the partial wetting regime. The necessary relationship between the base radius and the contact angle was established by the introduction of the spherical cap approximation. Experimental data for several liquid−solid systems were successfully fitted. The fitted parameters are physically meaningful and consistent with the microscopic properties of the liquids and solids. The hydrodynamic models, such as that of Voinov,[7] give an equally good fit to the experimental data but do not yield realistic values for the slip parameter. This suggests that additional dissipative processes are at work within the three-phase zone, which may not be omitted from the overall description. In the partial wetting regime, kinetic processes near the contact line determine the rate of contact angle relaxation and droplet spreading. Until a more general model of wetting dynamics is validated (such as that of Shikhmurzaev[21,22]), the molecular kinetic theory and conventional hydrodynamic models are perhaps best treated as complementary (as has been done by Petrov and Petrov[29]). For very viscous liquids and complete wetting, the equations of Voinov and Cox and the theoretical interpretation given by de Gennes are very useful. For partial wetting, the molecular-kinetic theory seems to be more appropriate.

Acknowledgment. This research is supported by the European Community with Grant CHRX-CT94-0448 and by the Ministère de la Région Wallonne. The support of Kodak European R & D is also acknowledged.

LA970825V

(28) Petrov, P. G.; Petrov, J. G. *Colloids Surf.* **1992**, *64*, 143.
(29) Petrov, P. G.; Petrov, J. G. *Langmuir* **1992**, *8*, 1762.